

# Centrifuge and numerical modelling of compensation grouting near tunnel linings

## Modélisation numérique et en centrifugeuse d'injection de compensation au voisinage de parement de tunnel

S.W.Lee, M.D.Bolton, R.J.Mair & K.Soga – *Cambridge University, Engineering Department, Trumpington Street CB2 1PZ, U.K.*  
 G.R.Dasari – *National University of Singapore*  
 T.Hagiwara – *Nishimatsu Construction Co.Ltd., Tokyo*

**ABSTRACT:** Compensation grouting aims to replace volume loss and prevent settlement caused by tunnelling. Whilst making injections to push the ground back up, it must be recognised that a downward reaction must be exerted which may deform the tunnel lining. Both centrifuge and numerical modelling have been carried out to investigate the effects of grouting depth, width, separation to the tunnel crown, and injection type on the surface heave and tunnel lining displacement. Results from tests on dense sand show that multiple-point widely spaced simultaneous injection is the ideal to which engineers should aspire in creating practical schemes.

**RÉSUMÉ:** L'injection de compensation a pour but de remplacer le volume de terrain perdu et d'empêcher le tassement induit par le creusement d'un tunnel. Tout en effectuant des injections afin de repousser le terrain vers le haut, il faut noter qu'un effort de réaction vers le bas doit être appliqué, celui-ci pouvant causer une certaine déformation du parement du tunnel. Une modélisation à la fois numérique et en centrifugeuse a été entreprise afin d'étudier l'impact de la profondeur, l'étendue, la distance au sommet du tunnel et le type d'injection, sur le gonflement en surface et le déplacement du parement du tunnel. Les résultats de tests sur sable dense montrent qu'un groupe d'injections multipoints, largement espacées et simultanées, représente le schéma idéal vers lequel les ingénieurs doivent tendre lors de la conception d'un programme d'injection.

### 1 INTRODUCTION

Compensation grouting is a novel technique used to mitigate or eliminate surface settlement caused by tunnelling. Grouting is usually carried out in three stages, as for the London Jubilee Line Extension project. Pre-treatment grouting is to compact the ground until heave is detected, concurrent grouting is to arrest settlement during tunnelling before it has a chance to affect overlying structures, and observational grouting is a remedial method for post excavation settlements. While doing compensation grouting, one must recognise that extra loads may be induced in the tunnel lining. This was listed by a report published by the UK Health and Safety Executive (HSE) (2000) as one of the factors which may have contributed to the collapse of New Austrian Tunnelling Method (NATM) tunnels at Heathrow Airport in 1994. Distortions of tunnel linings due to grouting pressures above a tunnel had been reported at the Bolton Hill Tunnel, USA (Zeigler and Wirth, 1982) and the Waterloo Station, London (T&T, 2000).

The effects on tunnel linings of compensation grouting become more profound if the linings are of segmental type where the joints are not full strength and where slippage of adjoining segments may occur. A Japanese tunnelling contractor, Nishimatsu Construction Co. Ltd., acknowledged this possible problem when they were using compensation grouting at the London Docklands Light Railway Lewisham Extension twin-tunnelling project (Lee et al. 1999). A research collaboration was therefore established between the contractor and the Geotechnical Group of Cambridge University to investigate the effects on a segmental tunnel lining of grouting depth, width, separation to the crown, and multiple-point injection either in simultaneous or sequential fashion. This research involved the use of both centrifuge and numerical modelling.

### 2 CENTRIFUGE and NUMERICAL MODELLING

Physical modelling was carried out at 1/75<sup>th</sup> scale with dry dense and loose sand in a container flying at 75g on the balanced beam centrifuge in the Schofield Centrifuge Centre of Cambridge Uni-

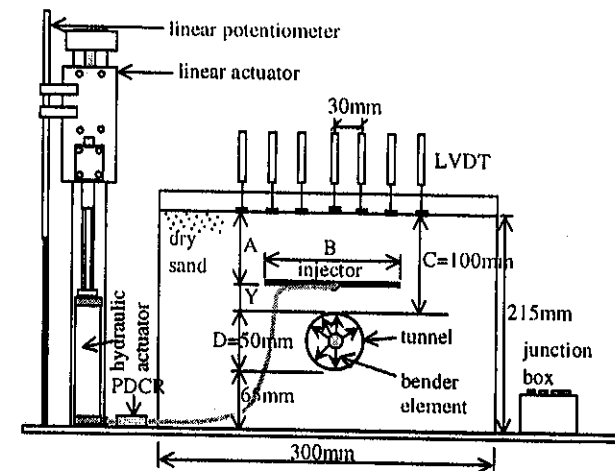


Figure 1. Centrifuge test set-up.

versity. For real grouting in cohesionless soil, the grout manifests itself as a bulb to displace, and coincidentally, to densify the surrounding soil without permeating into the soil pores. This is analogous to creating a 'balloon' or expansion in the soil. This concept was adopted in the centrifuge modelling where an expandable rubber sleeve with controllable injection volume simulated the compaction grouting, while the pressure of the injection could also be measured. The sand specimens comprised Leighton Buzzard sand, size 90-150µm, for which the critical state angle  $\phi_{crit}$  was 32°. A segmental model tunnel was constructed with bender elements inside it to measure the radial tunnel lining displacement at the segments and near to the joints. The surface heave was also measured. Figure 1 shows a centrifuge test set-up; more details can be found in Lee et al. (2001a).

Numerical modelling used a finite element analysis (FEA) package ABAQUS. The FEA mesh replicated the centrifuge test geometries and testing procedures. Analyses were carried out in plane strain condition as were the centrifuge tests. Two soil constitutive models were used, the critical state model with non-linear stiffness from small strain and the standard bilinear Mohr

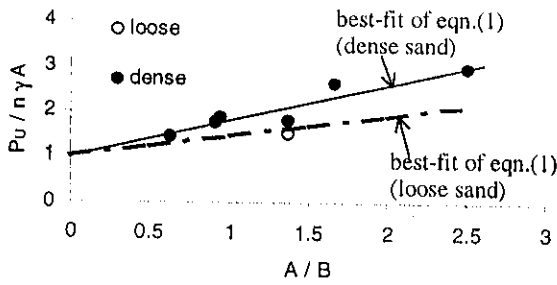


Figure 2.  $P_U/n\gamma A$  versus  $A/B$ .

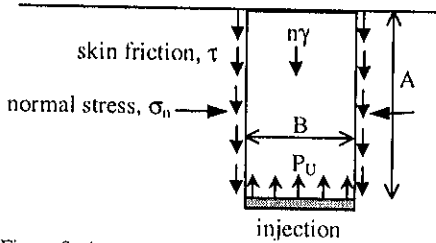


Figure 3. A proposed limit equilibrium analysis.

Coulomb model. Only results from the critical state model will be presented here. The procedures of the FEA and the definitions of the soil models can be found in Lee et al. (2000) and Lee et al. (2001b).

### 3 STRIP INJECTION

In total, six strip injection tests were carried out in dense sand and one in loose sand to investigate the effects of grouting depth  $A$ , width  $B$ , separation  $Y$ , pressure  $P$  and volume, vol. Figure 2 plots the maximum uplift resistance over overburden pressure ratio  $P_U/n\gamma A$  against the grouting depth over width ratio  $A/B$ . The  $P_U$  value is defined as the maximum grouting pressure that causes the break-out of the ground. Figure 3 shows a proposed limited equilibrium analysis for the uplift mechanism of soil subjected to grouting pressure. Resolving the forces vertically, it gives

$$\frac{P_U}{n\gamma A} = 1 + \frac{A}{B} (K \tan \phi) \quad (1)$$

where  $K$  is the coefficient of earth pressure and  $\phi$  is the soil friction angle. The parameter  $(K \tan \phi)$  is very similar to the skin friction coefficient,  $\beta$  ( $=K \tan \phi = \tau_s/\sigma'_v$ , ratio of skin friction to effective overburden) used in the calculation of the skin friction of piles.

The best-fit line of equation (1) on Figure 2 for the dense sand tests produces  $(K \tan \phi) = 0.79$ . The  $\phi_{max}$  value (assuming  $\phi = \phi_{max}$ ) is then determined as  $49.5^\circ$  from Bolton (1986) using equation:

$$\phi_{max} = \phi_{crit} + A [J_u I_c - 1] \quad (2)$$

where parameter  $A$  can be taken as  $5^{I_D}$  in plane strain,  $I_D$  is the relative density ( $=0.9$  for centrifuge dense sand), and  $I_c$  is the relative crushability which can be taken as 5 at low stress level ( $<150\text{kN/m}^2$ ). This generates a corresponding  $K$  value of 0.67. A similar approach can be used for the loose sand test, where  $\phi_{max}$  is calculated as  $33.7^\circ$  taking  $I_D=0.27$ . The  $(K \tan \phi)$  value is then calculated as 0.45 using the same value  $K=0.67$  as that determined for the dense sand tests. This enables equation (1) for loose sand to be plotted on Figure 2, and the line falls close to the point of the loose sand centrifuge test. The justification of using this unique  $K$  value via FEA can be found in Lee (2001c).

Figure 4 shows a distorted mesh of FEA for grouting pressure on a strip injection test in dense sand ( $A=75\text{mm}$ ,  $Y=25\text{mm}$  and  $B=55\text{mm}$ ). Directly above and beneath the grouting strip soil undergoes compression, and above the edges of the grouting strip soil undergoes shearing. Near to the centreline soil elon-

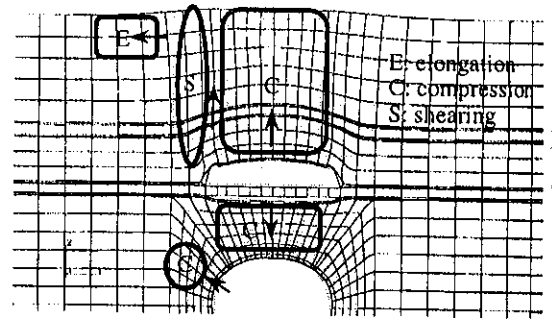


Figure 4. Zone of soil deformation due to grouting pressure.

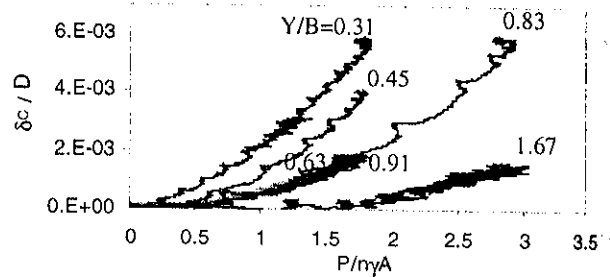


Figure 5.  $\delta_{c,U}/D$  versus  $P/n\gamma A$  as dependent of ratio  $Y/B$ .

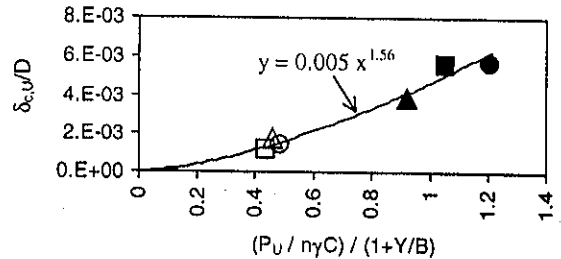


Figure 6. Dependence of  $\delta_{c,U}$  on  $P_U$  and grouting geometries.

gates in the horizontal direction, but at the edges of the heaving block soil is squeezed in the horizontal direction and extends vertically. Beneath the injection the soil compresses vertically and presses on the tunnel crown which also causes the tunnel shoulders to press outwards and compress the soil.

The tunnel lining displacement is found to be dependent on the grouting pressure, volume and geometries. Figure 5 shows the ratio of tunnel crown inwards displacement over tunnel diameter ( $\delta_{c,U}/D$ ) against the normalised grouting pressure  $P/n\gamma A$  as dependent on the grouting separation over width ratio  $Y/B$ . A smaller  $Y/B$  ratio, which means a closer separation or a wider grouting width, displaces the tunnel crown more. The maximum crown displacement is delimited when the  $P_U$  point is reached due to the limited grouting pressure. A simple grouting pressure transfer mechanism (Lee et al., 2001a) enables the maximum crown displacement,  $\delta_{c,U}$  to be related to  $P_U$  and the grouting geometry as

$$\frac{\delta_{c,U}}{D} \propto \frac{P_U}{n\gamma C} \frac{1}{\left(1 + \frac{Y}{B}\right)} \quad (3)$$

Figure 6 shows that the  $\delta_{c,U}$  data plotted according to equation (3) can be fitted by a power law curve with modest scattering.

### 4 MULTIPLE-POINT SIMULTANEOUS INJECTION

In multiple-point injection, three injectors of the same size were used, see Figure 7. The total width of the array of injectors,  $B'$  was maintained at 80mm. Two tests at grouting widths  $B$  of

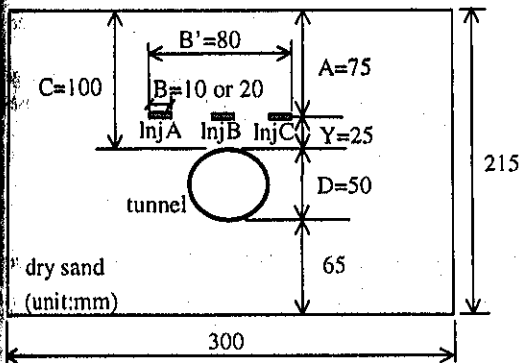


Figure 7. Multiple-point injection test set-up.

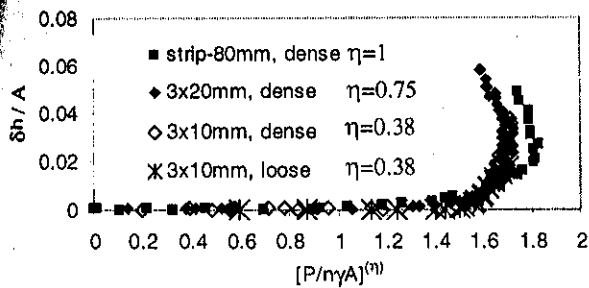


Figure 8.  $\delta h/A$  versus  $[P/nyA]^m$ .

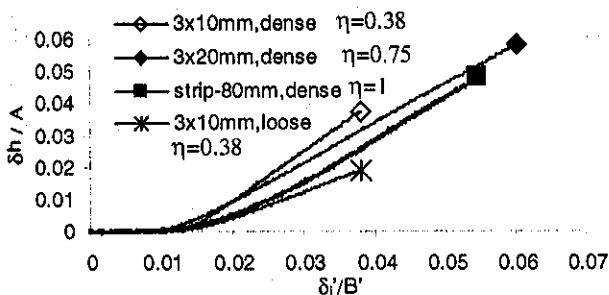


Figure 9.  $\delta h/A$  versus  $\delta_i'/B'$  for different  $\eta$  values.

10mm and 20mm were carried out in dense sand and one test with  $B=10$ mm in loose sand, all were at grouting depth  $A=75$ mm. For simultaneous injection, the three injectors were expanded at the same time.

Figure 8 shows the ratio of centre surface heave over grouting depth ( $\delta h/A$ ) against the normalised grouting pressure  $P/nyA$  to the power of grouting coverage  $\eta (=mB/B')$ , where  $m$  is the number of injectors. It can be seen that the multiple-point injection data can be grouped together and fall close to the data of a strip injection test having  $B=80$ mm, i.e.  $\eta=1$ . When the ratio  $\delta h/A$  is plotted against the normalised grouting thickness  $\delta_i'/B'$ , a smaller  $\eta$  value creates more centre surface heave, see Figure 9. The parameter  $\delta_i'$  is the grouting thickness and defined as the grouting volume over the plan area of the array of injectors. The test in loose sand obviously undergoes compression due to grouting pressure and creates less heave.

## 5 MULTIPLE-POINT SEQUENTIAL INJECTOR

In multiple-point sequential injection, the three injectors were expanded in dense sand in three different sequences, namely, left(InjA)→centre(InjB)→right(InjC), centre→left→right, and right→left→centre, see Figure 7. One test with the injection sequence of left→centre→right was repeated in loose sand. A typical example of grouting pressure,  $P$ , versus total grouting volume,  $vol_T$ , is shown in Figure 10. At the instant of closing an injector and opening another one there is an instantaneous in-

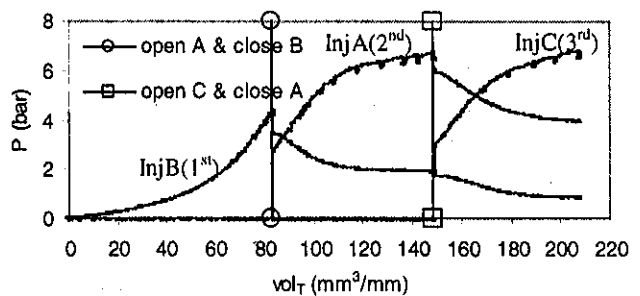


Figure 10. Increase and decrease of injector pressure at the instant of opening injector valves.

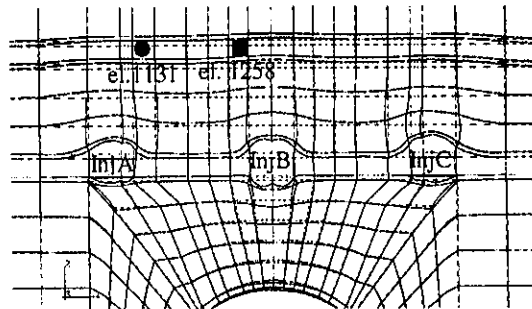


Figure 11(a). FEA mesh and element locations.

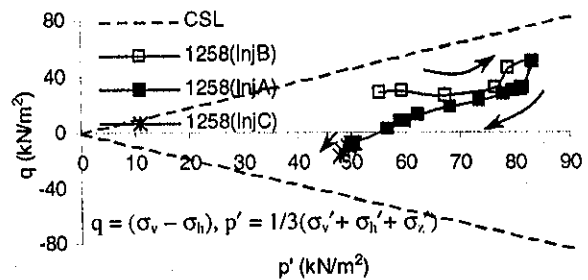


Figure 11(b). Stress path for element 1258.

crease of grouting pressure at the opened injector and decrease in the previous injector. This is due to the new injector which requires some small inflow of water to reach its pressure, and to the sharing of uplift force between the larger number of injectors.

Figure 11(a) shows the FEA stress paths (injection sequence of centre(InjB)→left(InjA)→right(InjC)) undergone by two soil elements above the injection points. At the first injection (InjB), element 1258 suffers from vertical compression loading, see Figure 11(b). At the same time, element 1131 (Figure 11(c)) compresses horizontally. The second injection at InjA causes element 1258 to experience vertical unloading. On the other hand, element 1131 shows vertical compression loading towards the critical state line, CSL. The cyclic stress paths undergone by these two soil elements will cause compression of the soil (Tatsuoka & Ishihara, 1974) and also increase its stiffness. The third injection at InjC is far enough from elements 1258 and 1131 to create negligible effect.

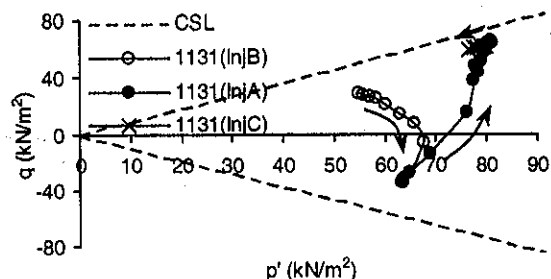


Figure 11(c). Stress path for element 1131.

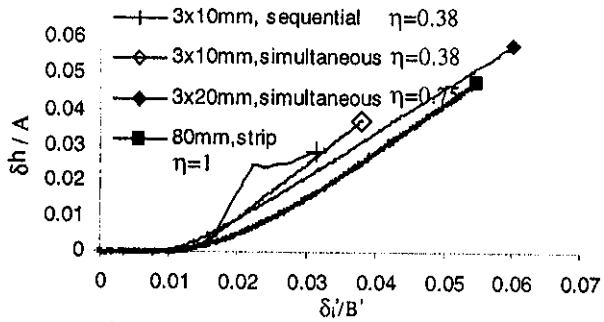


Figure 12.  $\delta h/A$  versus  $\delta_i/B'$  for different injection types having  $B'=80\text{mm}$  and  $A=75\text{mm}$ .

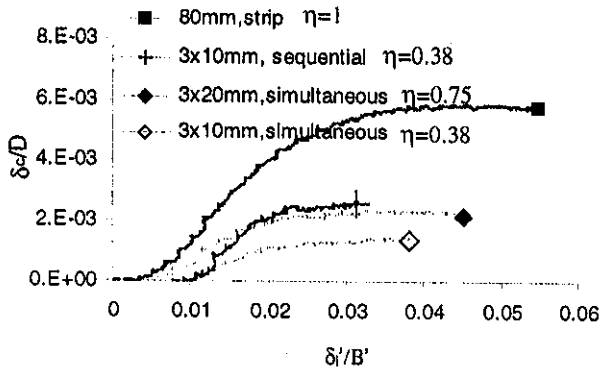


Figure 13.  $\delta_c/D$  versus  $\delta_i/B'$  for different injection types having  $B'=80\text{mm}$  and  $A=75\text{mm}$ .

## 6 DISCUSSION and CONCLUSIONS

It is useful to compare the centre surface heave and the tunnel crown inwards displacement against the normalised grouting thickness for all types of injections having the same  $B'$  and  $A$  values, and sand density. Figure 12 reveals that the sequential injection (left→centre→right) creates the most favourable centre surface heave  $\delta h/A$ , but at higher  $\delta_i/B'$  ratio ( $\approx 0.03$ ) it approaches the heave generated by the simultaneous injection for which  $\eta=0.38$ . The strip injection test gives the lowest heave. Figure 13 reveals that the strip injection creates the most tunnel crown displacement  $\delta_c/D$  and the simultaneous injection with  $\eta=0.38$  creates the least. In compensation grouting, the main objective is to create more surface heave and smaller tunnel lining displacement for an injection volume. The centrifuge tests suggest the use of multiple-point simultaneous and sparse injection as the best option to meet these two criteria.

The conclusions are as follow:

- The surface heave is dependent on the overburden pressure, and the ratio of grouting depth over width ( $A/B$ ), with a smaller ratio lifting the ground earlier.
- The tunnel lining displacement is dependent on grouting pressure, volume or thickness, and the ratio of grouting separation over width ( $Y/B$ ), with a smaller ratio creating more lining displacement.
- The maximum tunnel crown displacement in different grouting geometries can be assessed using equation (3) with respect to the maximum grouting pressure  $P_U$ .
- With multiple-point simultaneous injections, an exponent of coverage ratio,  $\eta$ , applied to the normalised grouting pressure, groups the centre surface heave data. A smaller  $\eta$  ratio is preferred as it creates more surface heave and smaller lining displacement for a given injection volume.
- With multiple-point sequential injection, the soil compression and stiffening effects caused by cyclic stresses and strains result in higher subsequent grouting pressures. This helps in

generating more surface heave, but also creates more tunnel lining displacement.

Multiple-point simultaneous injection with a lower coverage  $\eta$  ratio is the best option to meet the objectives of compensation grouting, based on these centrifuge results.

## REFERENCES

- Bolton, M.D. 1986. The strength and dilatancy of sands. *Geotechnique*: 36, No.1, pp. 65-78.
- HSE (Health & Safety Executive, UK) 2000. The collapse of NATM tunnels at Heathrow Airport. *HSE BOOKS*. ISBN 0 7176 17920
- Lee, S.W., Dasari, G.R., Mair, R.J., Bolton, M.D., Soga, K., Sugiyama, T., Ano, Y., Hagiwara, T. & Nomoto, M. 1999. The effects of compensation grouting on segmental tunnel linings. *Geotechnical Aspect of Underground Construction in Soft Ground*, Tokyo, July, pp. 257-262.
- Lee, S.W., Bolton, M.D., Mair, R.J., Soga, K., Dasari, G.R., & Hagiwara, T. 2000. Modelling of injection in sand. *International Conference on Tunnels and Underground Structures*, Zhao, Shirlaw & Krishnan (eds), Singapore, pp. 665-670.
- Lee, S.W., Bolton, M.D., Mair, R.J., Hagiwara, T., Soga, K. & Dasari, G.R. 2001a. Centrifuge modelling of injection near tunnel lining. *International Journal of Physical Modelling in Geotechnics*, Vol. 1, No.1, March, pp. 9-24.
- Lee, S.W., Bolton, M.D., Mair, R.J., Soga, K., Dasari, G.R., & Hagiwara, T. 2001b. Soil models and stress paths on injection in sand. *Regional Conference on Geotechnical Aspects of Underground Construction in Soft Ground*, Shanghai, April, in press.
- Lee, S. W. 2001c. The effects of compensation injections on tunnels. *PhD thesis*, Cambridge University, to be submitted.
- Tatsuoka, F. & Ishihara, K. 1974. Drained deformation of sand under cyclic stresses reversing direction. *Sails and Foundations*: Vol. 14, No. 3, pp. 51-65.
- T&T (Tunnels & Tunnelling International) 2000. JLE and the lessons from Heathrow. June, vol.32, No.6, pp. 41-44.
- Zeigler, E.J. & Wirth, J.L. 1982. Soil stabilisation by grouting on Baltimore Subway. *Proc. of Conf. on Grouting in Geotechnical Engineering*, New Orleans, ASCE, pp. 576-590.